Bulletin of Earthquake Engineering (2024) 22:4197–4217
https://doi.org/10.1007/s10518-024-01932-x

ORIGINAL ARTICLE

Seismic performance assessment of an existing anchored and a self-anchored liquid storage tank in high seismic regions

Bulent Erkmen[1]

Received: 26 February 2024 / Accepted: 8 May 2024 / Published online: 15 May 2024
© The Author(s) 2024

Abstract
This study presents seismic performance of two existing at-grade industrial liquid-storage tanks located in the Eastern part of Marmara region, which is a high seismic region in Turkey. The first tank is self-anchored (unanchored) and has been in service for 44 years, while the other tank is mechanically anchored to a reinforced concrete foundation and has been in service for 50 years. Tanks seismic performance is evaluated using tank time-history earthquake analyses with recorded ground motions scaled for each tank site. The liquid content was included in the developed model using provisions of API 650. Tanks base uplift, sliding on the foundation, tank shell and bottom plate damage, and demand on tank anchorage were determined. The results shows that self-anchored tank has base plate uplift and sliding that are larger than the allowable limits while the mechanically anchored tank has acceptable seismic performance with potential seismic damage of tank anchorage system. The findings of this study contribute valuable insight into the seismic performance of existing liquid storage tanks in the region under new seismic regulations and increased seismic loads than those used for their design.

Keywords Self-anchored tank · Mechanically anchored tank · Liquid-storage tank · Tank base uplift · Fluid-structure interaction

1 Introduction

At-grade liquid storage tanks play a vital role in modern industrial facilities and public water supply system. Ensuring a reliable and safe water supply system is essential for post-earthquake firefighting and preventing outbreak of diseases resulting from the lack of clean water and proper sanitation facilities for earthquake survivors. Liquid storage tanks often store a variety of hazardous substances, including petrochemical products

✉ Bulent Erkmen
bulent.erkmen@ozyegin.edu.tr

[1] Department of Civil Engineering, Ozyegin University, Istanbul, Turkey

such as crude oil, gasoline, fuel oil, diesel, LPG, and hydrochloric acid, as well as industrial chemicals such as styrene and ammonia, along with food processing liquids. The failure of at-grade liquid storage tanks has often led to release of toxic materials to enviorement, causing catastrophic consequences such as fires and explosions, as seen in reviewed 242 accidents of storage tanks that occurred in industrial facilities over last 40 years (Chang and Lin 2006). The seismic performance of liquid storage tanks is a matter of special importance, extending beyond the economic value of the tanks and their contents. Therefore, it is crucial to ensure seismic resilience of liquid-storage tanks in earthquake prone regions. However, liquid storage tanks were reported to have significant damage following the 1979 Imperial Valley earthquake (Haroun 1983; Shih and Babcock 1984), the 1983 Coalinga earthquake (Manos and Clough 1985), the 1994 Northridge earthquake (Caprinozzi et al. 2020), the 1995 Hanshin (Kobe) earthquake (Çelik and Köse 2020), and 1999 Kocaeli (Izmit) earthquake (Girgin 2011; Men et al. 2024; Scawthorn and Johnson 2000).

The seismic behavior of liquid storage tanks varies significantly from that of traditional structures. This distinction arises not only from the interaction between the liquid and the structure but also from multiple sources of nonlinear behavior, including tank shell deformation, liquid sloshing, nonlinear interaction between the tank and the supporting soil, material yielding and buckling, and repeated contact and separation between the tank base and its foundation (Ozdemir et al. 2010). Initial analyses of liquid storage tanks were done under the assumption that the tank was rigid and fully anchored to a rigid foundation (Housner 1957, 1963; Jacobsen 1949). Subsequent studies considered the flexibility of the tank wall and revealed its significant impact on the dynamic response of liquid storage tanks (Veletsos and Auyang 1977; Haroun and Housner 1981; Haroun 1983). Recent research efforts have focused on effects of ground flexibility and its coupling with the vibrating tank system, base isolation, tank base uplift, various analysis methods, and experimental investigations (Malhotra 1995; Ormeño et al. 2015, 2019; Vathi and Karamanos 2015; Rawat and Matsagar 2022; Zhu et al. 2023).

Although new computational methods, such as modelling the liquid content with fluid elements like Coupled Eulerian/Lagrangian (CEL) method and Smoothed Particle Hydrodynamics (SPH), are gaining popularity, these methods increase the complexity of the finite element model and in turn increases the computational cost (Spritzer and Guzey 2017). The seismic design provisions for liquid storage tanks, such as those outlined in American Petroleum Institute (API) 650 (2020), are based on spring-mass analogy, also known as the mechanical mode or lumped mass model, developed for flexible tanks. This analogy considers a portion of the liquid mass to act as if rigidly linked to the tank walls, while the remaining portion of the liquid content is flexibly attached to the tank walls. The liquid that synchronizes with the tank vibration is known as the impulsive component, while the sloshing component of the liquid, which is attached to flexible tank walls, generates free surface waves, and has its own frequency of vibration, is referred to as the convective or sloshing component. The period of oscillation for the free surface sloshing component is typically significantly longer than the fundamental period of the impulsive liquid-tank system. This spring-mass analogy modelling approach has been widely used to study seismic performance of liquid storage tanks (Chaulagain et al. 2018; Goudarzi 2020; Hernandez et al. 2021; Kalantari et al. 2019; Malhotra et al. 2000).

Turkey is situated in one of the most seismically active regions (Girgin 2011; Scawthorn and Johnson 2000; Sezen and Whittaker 2004). The devastating 2023 Kahramanmaras (Turkey) earthquakes, which had a moment magnitude of 7.7 and 7.6, impacted over 14 million individuals, resulting in an official death toll exceeding 50,000 (Altunsu et al. 2024). The seismic events caused extensive damage to various civil infrastructures, including buildings, government offices, dams, airports, and roads. Similarly, the 1999 Kocaeli earthquake, with a moment magnitude of 7.4, had a profound impact on the heavy industry situated close to the North Anatolian fault, which ruptured during the earthquake. This earthquake caused significant destruction including tank failures, release of toxic materials, and tank fires that continued for several days (Scawthorn and Johnson 2000; Sezen and Whittaker 2004).

This study investigates seismic performance of two industrial at-grade liquid-storage tanks situated near the North Anatolian fault in the Marmara region of Turkey. The first tank is self-anchored and has been in service for 44 years, while the other tank is mechanically anchored to its foundation and has been in service for 50 years. Seismic performance of the tanks is evaluated using field measured geometric properties as well as available limited construction documents. The seismic time history analyses performed account for both material and geometric nonlinearity and tank foundation dynamic interaction including sliding and base uplift under eleven recorded ground motions for each tank site. The findings of this study offer a detailed case study on the seismic performance of existing industrial liquid-storage tanks that were designed based on historical codes and seismic standards.

2 Properties of tanks

Two liquid storage tanks were selected for the case study. Tank-A, a self-anchored steel tank, is located near Kocaeli, Turkey. Tank-A is used to store styrene, which is a flammable liquid that can release toxic fumes when burned and can be explosive in certain circumstances. The tank is fabricated in early 1980s, but there is limited information available regarding its design basis. The tank, shown in Fig. 1, has a diameter of 10.69 m and height of 12.4 m with a 1.0 m roof height.

Tank-A including walls (shell courses), bottom plate, and roof is fabricated using steel grade S235, which is a typical steel grade for liquid storage tanks due it is weld-

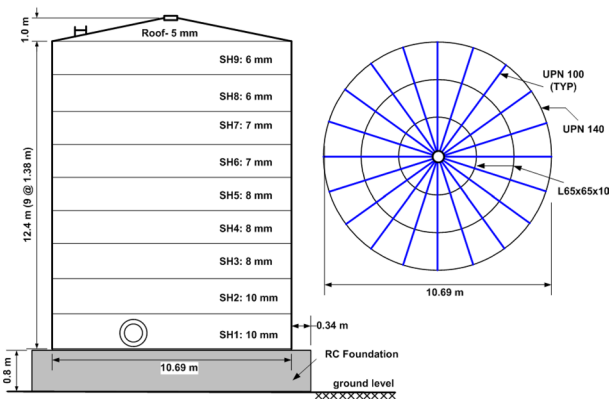


Fig. 1 Geometry of self-anchored tank (Tank-A front view and roof framing)

ability and ductility. The tank is constructed using nine shell courses, with thickness varying from 10 mm at tank bottom to 6 mm at the top. The tank roof is fixed dome-shaped roof, constructed with 5 mm thick plate supported by UPN 100 rafters spaced at 18-degree intervals. Additionally, L65 × 65 × 10 angle sections are utilized as ring frame members, with UPN140 functioning as the top wind girder for added structural stability. The tank bottom plate was field measured to be 13 mm thick, and it rests on a reinforced concrete foundation approximately 0.8 m thick. The tank is unrestrained and free to slide across the foundation, lacking any mechanical connection or anchors between the tank and its foundation. However, the nominal clearance of only 0.34 m between the tank wall and elevated foundation edge poses a significant risk of tank failure and stability if the tank slides more than 0.34 m in the event of an earthquake as shown in Fig. 1.

Tank-B, a mechanically anchored steel tank, is situated near Gemlik, Turkey. The tank is 34.0 m in diameter and 33.78 m in height with a 2.0 m roof height as shown in Fig. 2. The tank design liquid filling height is 32.3 m, and it is used to store liquid ammonia, which is a hazardous chemical compound with potential to explode, posing serious safety risks to individuals and the surrounding environment. Typically, ammonia is stored at temperatures below its boiling point of -33 degrees Celsius at atmospheric pressure. Therefore, the tank walls and roof are fully covered with insulation material to keep ammonia in liquid form.

The tank, designed and fabricated in 1974 following API 620 standards (API 1970), has a design wind speed of 161 km/hr. The seismic design lateral load is equal to 6% of tank total weight including the liquid and insulation weights. The total lateral seismic load is distributed as an inverse triangular load, a design approach that differs significantly from the modern seismic design provisions used for liquid storage tanks. The tank is constructed using 15 shell courses with thickness ranging from 24.8 mm at the bottom course to 6.35 mm for the top shell course. The tank roof is fixed doom-shaped, constructed with 4.8 mm steel plate. All plate thickness values are based on field measurements done using ultrasonic testing as well as construction and maintenance documents. The 4.8 mm thick roof plate is supported by a framing system comprised of IPE 220 rafters spaced at 10-degree intervals and L80 × 80 × 8 angle sections serving as ring framing. At the connection of the roof plate and top shell course, 49.5 mm plate

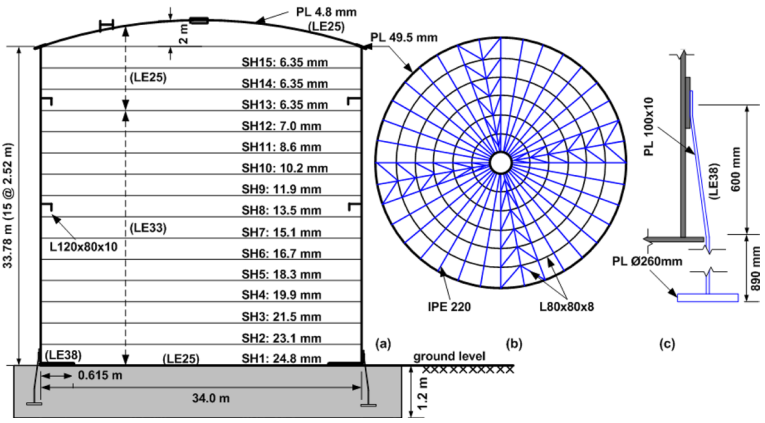


Fig. 2 Geometry of mechanically anchored tank (Tank-B) (**a**) front view, (**b**) roof framing, and (**c**) foundation anchor

is utilized as top wind girder, while two L120×80×10 angle sections are employed as intermediate wind girders to enhance tank stability. The tank bottom annular plate has a radial width of 0.615 m and a thickness of 10 mm, while the tank bottom plate is 6.36 mm thick. The tank is secured to its reinforced concrete foundation using 24 anchor plates, each measuring 100×10 mm, as shown in Fig. 2. These anchor plates are embedded in the foundation reinforced concrete, which has compressive strength of 25 MPa.

The tank design documents provide detailed information on the steel material properties for plates and roof framing, including data on yield strength, ultimate strength, and fracture strain. Three steel grades, namely LE25, LE33, and LE38, are utilized for the tank components. The LE25 and LE33 grades are used for the tank shell courses, roof plate, and bottom plate. The roof IPE 220 rafters are fabricated from LE25, while the angle sections and anchorage plates are LE38. The yield strengths of LE25, LE33, and LE38 are 245 MPa, 324 MPa, and 373 MPa, while their ultimate strength and fracture strains are 392 MPa, 471 MPa, and 530 MPa, with corresponding strain values of 0.28, 0.24, and 0.22, respectively. The stress-strain data used for each steel grade, as derived from the available data, is shown in Fig. 3.

Tank-B is a large diameter liquid storage tank that is in service for almost 50 years. The tank is storing ammonia at a temperature below its boiling point of -33 degrees Celsius, which is much smaller than ambient temperature in the tank site throughout the year. Therefore, there was a need to determine tank geometric imperfections or in this case deformations due to operation. For this purpose, field measurements were performed according to API 653 (2014) at 16 radial stations (22.5 degrees) on tank wall in the vicinity of tank bottom and 3.0 m below the tank wall-roof connection. The geometric imperfections scaled by a factor of 20 are shown in Fig. 4. The average geometric imperfection at wall-roof connection region was 13 mm with a maximum value of 106 mm. These geometric imperfections were considered for the developed finite element model of the tank by modifying the coordinates of nodes corresponding to the station points according to the measured imperfections. The numerical study performed by

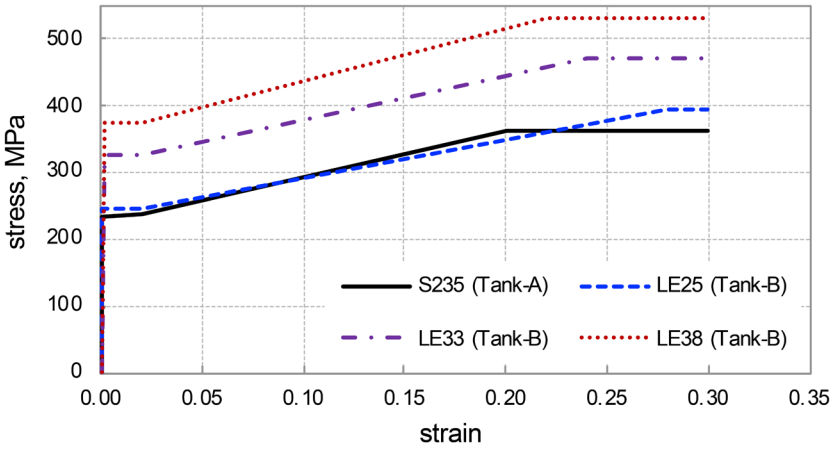


Fig. 3 Stress-strain curves for steel grades used for Tank-A and Tank-B

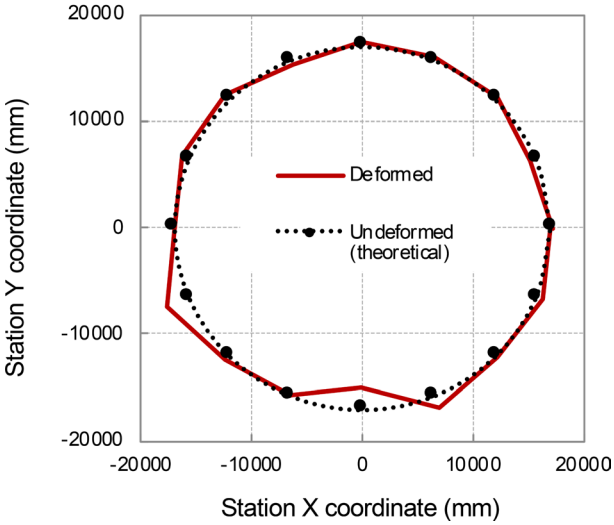


Fig. 4 Geometric imperfections of Tank-B (scaled by a factor of 20)

Spritzer et al. (2019) showed that tanks with imperfections within the API 650 (2020) tolerances exhibit minimal deviation from the ideal tank condition. Tank-B measured imperfections fall within the API 650 maximum out-of-plumbness limit for the tank top shell, which is 1/200 of the total tank height. The corresponding imperfection limit at the location where the imperfections are measured is 154 mm. Therefore, the measured imperfections are unlikely to have a significant impact on the seismic behavior of the tank. For Tank-A geometric imperfections are not considered to be significant based on field inspections and due to its relatively smaller dimensions.

3 Numerical analyses of the tanks

3.1 Analytical models

The seismic design provisions of API 650 (2020) for liquid storage tanks, which are based on spring-mass analogy or lumped mass model shown in Fig. 5 are used to model liquid content of the tanks. The required parameters for defining convective and impulsive liquid components include liquid masses, the periods of their fundamental vibration modes, and locations of mass along the tank height. Once the period and mass of the liquid components are determined, the spring constant or stiffnesses can be calculated by utilizing the corresponding period and mass values.

The viscous damping of sloshing water is commonly set at 0.5% per API 650, while the impulsive component is typically 2% for steel tanks. In this study, the damping values for both convective and impulsive components are conservatively taken as 0.5% since damping sources such as tank sliding, uplifting and tank base hitting to the ground after uplift under reversal loading are explicitly modelled in the developed 3D tank FE models.

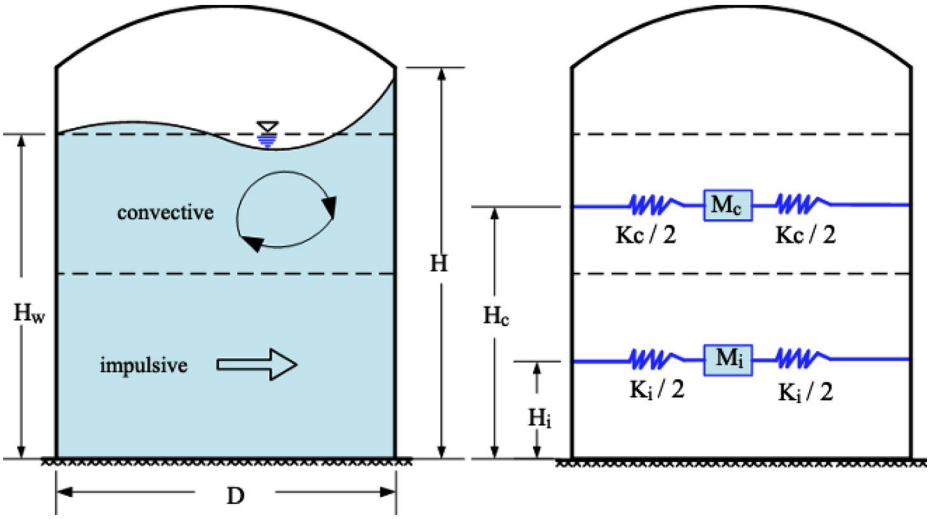


Fig. 5 Convective and impulsive liquid contents and mechanical model

For tanks where $D/H_w < 1.333$, the impulsive and convective liquid weights W_i and W_c along with their corresponding masses M_i and M_c are calculated as a fraction of the total liquid weight W_p through the following relationship.

$$W_i = \left(1 - 0.218\frac{D}{H_w}\right) W_p \tag{1}$$

$$W_c = 0.230\frac{D}{H_w}\tanh\left(\frac{3.67H_w}{\mathrm{D}}\right)W_p$$

The center of action for the effective lateral liquid forces, denoted as H_i and H_c is calculated as:

$$H_i = \left(0.5 - 0.094\frac{D}{H_w}\right) H_w \tag{2}$$

$$H_c = \left[1.0 - \frac{\cosh\left(\frac{3.67H_w}{D}\right) - 1}{\frac{3.67H_w}{D}\sinh\left(\frac{3.67H_w}{D}\right)}\right] H_w$$

The impulsive and convective liquid natural vibration periods T_i and T_c are calculated as:

$$T_i = \left(\frac{1}{27.8}\right)\left(\frac{C_i H_w}{\sqrt{t_u/D}}\right)\left(\sqrt{\frac{\rho}{E}}\right) \tag{3}$$

$$T_c = 1.8\left[\frac{0.578}{\sqrt{tanh\left(\frac{3.68H_w}{D}\right)}}\right]\sqrt{\mathrm{D}}$$

Where coefficient C_i, which depends on H_w and D, is a dimensionless parameter, t_u is equivalent uniform thickness of tank shell, E is the elastic modulus of the tank material, and ρ is fluid density. The spring stiffnesses K_i and K_c are computed using the general relationship between mass, period, and stiffness. A summary of tanks seismic parameters for liquid content is given in Table 1.

3.2 Tank finite element models and earthquake analysis

The nonlinear time-history earthquake analysis of the tanks is performed using finite element code ABAQUS (2021), which is selected for its computational efficiency for modelling nonlinear contact (sliding and uplift over the base) as well as its stability for nonlinear time history analysis. The tank models include three main FE parts: the tank part, which includes shells, bottom plate, and roof plate; the roof frame part; and the rigid foundation part, as shown in Fig. 6. The assumption of rigid foundation is based on the presence of reinforced concrete mat foundations with thickness of 0.8 m for Tank-A and approximately 1.2 m for Tank-B. The rigid foundation modelling approach is in line with current construction practice, as noted by Bakalis and Karamanos (2021).

The FE model developed for Tank-A is shown in Fig. 6. The tank shells and foundation are modelled using S4R shell elements, a 4-node general-purpose shell element with reduced integration. This element is well-suited for conducting large strain analyses on both thin and thick shells. The roof framing and wind girder are modelled using two-node B31 Timoshenko beam elements, which are first-order shear-deformable beam elements suitable for analyzing both thick and slender beams. Tank-A FE model is meshed using a nominal mesh size of 300 mm. However, the tank base plate and foundations are meshed using a finer mesh size in the vicinity of tank perimeter where the tank is expected uplift under earthquake loads as shown in Fig. 6. The same mesh

Table 1 Summary of tanks seismic parameters for liquid content

Parameter	Unit	Tank-A	Tank-B
D	*m*	10.7	34.0
H_w	*m*	11.6	32.3
ρ	kg/m^3	906	682
t_u	*mm*	7.8	16.0
C_i	-	6.27	6.13
M_p	*mt*	944.7	19,993
M_i	*mt*	754.7	15,405
H_i	*m*	4.79	12.95
K_i	*kN/m*	150,618	357,008
T_i	*sec*	0.45	1.3
M_c	*mt*	200.3	4,831
H_c	*m*	8.79	23.59
K_c	*kN/m*	674	5109
T_c	*sec*	3.4	6.1

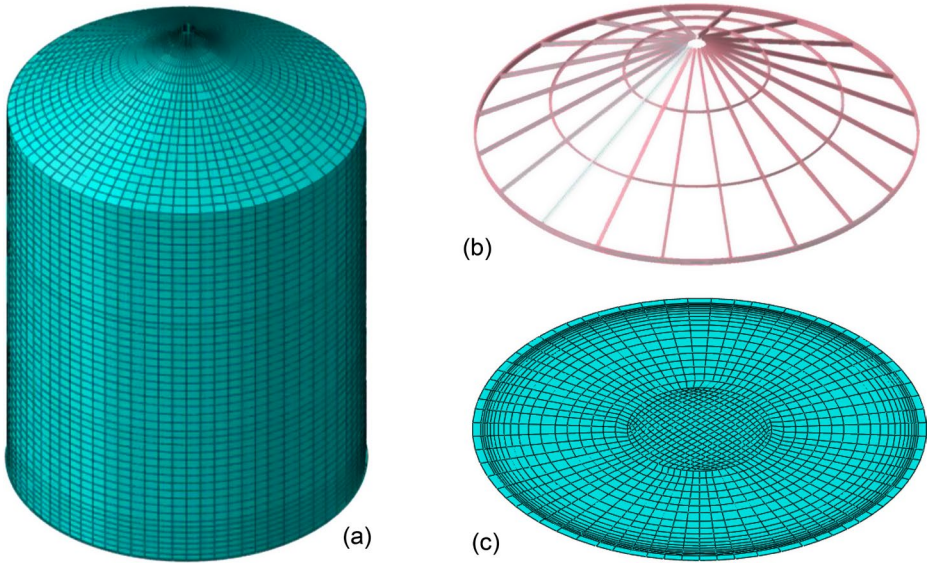


Fig. 6 Tank-A model parts and mesh (**a**) tank shell (**b**) roof frame (**c**) foundation and base plate

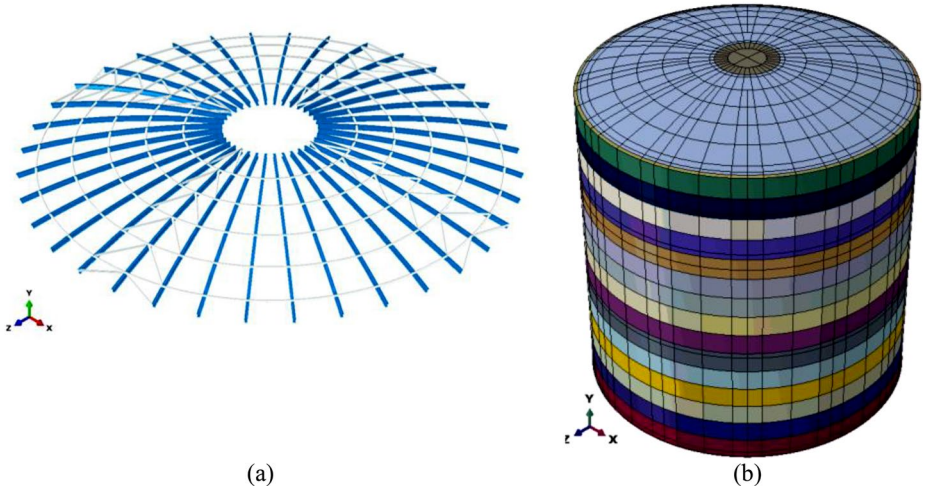


Fig. 7 Tank-B model parts (**a**) roof framing (**b**) tank shell plates

was used for both foundation and tank base plate to ensure improved sliding and uplift prediction of the tank under earthquake loads.

Figures 7 and 8 show Tank-B finite element model, comprising the roof framing, tank shell, tank foundation and tank base anchorage. The roof framing is modelled using B31 elements, while the tank plates are modelled using S4R shell elements. The 24 tank base

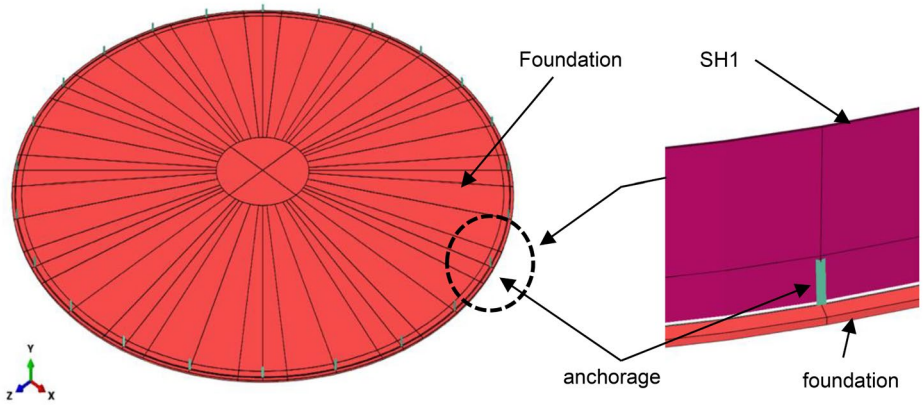


Fig. 8 Tank-B foundation and tank anchorage details

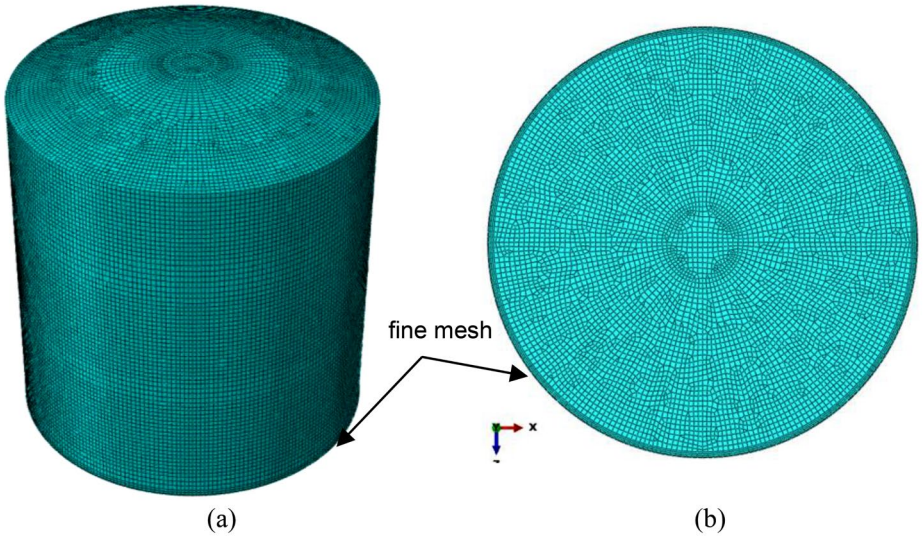


Fig. 9 Tank-B mesh (**a**) tank shell and roof (**b**) foundation and tank base plate

anchorages are modelled as beam elements (B31), which share the same nodes with the foundation for displacement compatibility at the foundation attachment points under earthquake loads. Additionally, at the tank SH1 wall course, the anchorage beams are connected to the shell course using "tie" constraint to model the connection between the tank wall and anchorage plate.

Figure 9 shows the meshed Tank-B model. A nominal mesh size of 400 mm is used for the tank, roof framing, and foundation. However, a finer mesh of 200 mm is used in the vicinity of the tank-foundation connection region to capture tank deformation and

tank-foundation interaction in this critical area. The anchorage beams are meshed with a nominal mesh size of 200 mm.

The earthquake analysis for both tanks is conducted using a static analysis step followed by a subsequent implicit dynamic analysis step, considering the material and geometric (second order) nonlinearity of the deforming tank. In the initial static step, the tank self-weight, insulation, other nonstructural weights, and liquid static hydrodynamic pressures are applied as shown in Fig. 10. The insulation applied to the walls and roof of Tank-B as non-structural mass is approximately 4.1 kg/m^2, whereas Tank-A does not have any insulation.

The effective impulsive and convective (sloshing) portions of the liquid seismic masses are attached to the tank wall at their calculated center of action using two reference points (RP) as shown in Fig. 11. These two reference points are connected using the corresponding springs for the two liquid masses and their fundamental vibration period. The RP-1 is connected to the tank walls through coupling constraint, while RP-2, where the liquid masses are assigned, is restrained for all degrees of freedom except for the displacement along the spring line of action, which is ground motion direction.

The interaction between Tank-A and its foundation is crucial, particularly because Tank-A is self-anchored and has potential to slide and uplift over the foundation. The interaction between the tank base plates and foundations is simulated through contact interaction. Following API 650 provisions, a static and dynamic friction coefficient of 0.40 is used conservatively. The contact formulation permits the separation of two surfaces, enabling the tank to uplift when the overturning moment exceeds the restoring moment. Even though Tank-B is designed not to uplift and slide on the foundation, still the same contact interaction is defined between the tank base plate and its foundation to account for any potential effects of tank sliding and lifting on tank anchorage system.

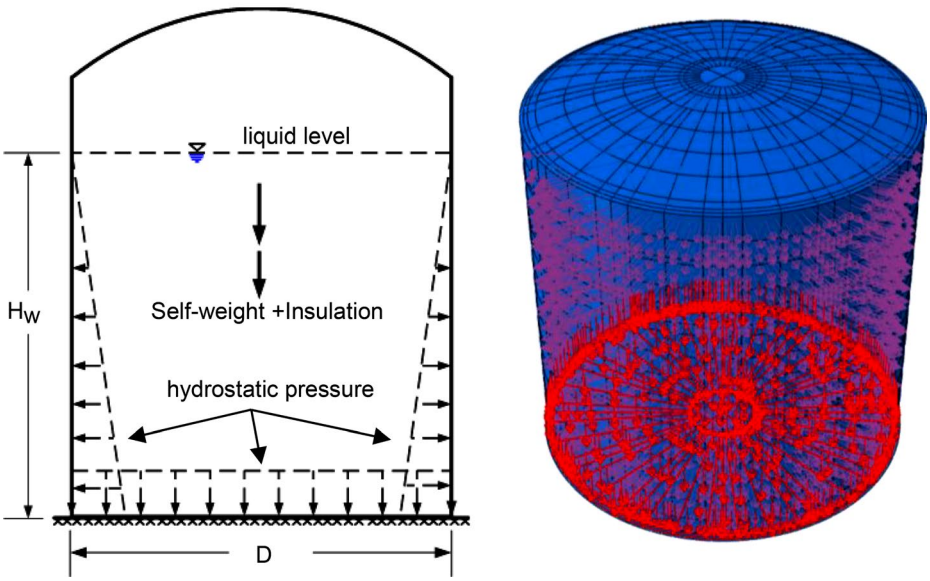


Fig. 10 Application of self-weight, other nonstructural weights, and hydrostatic loads

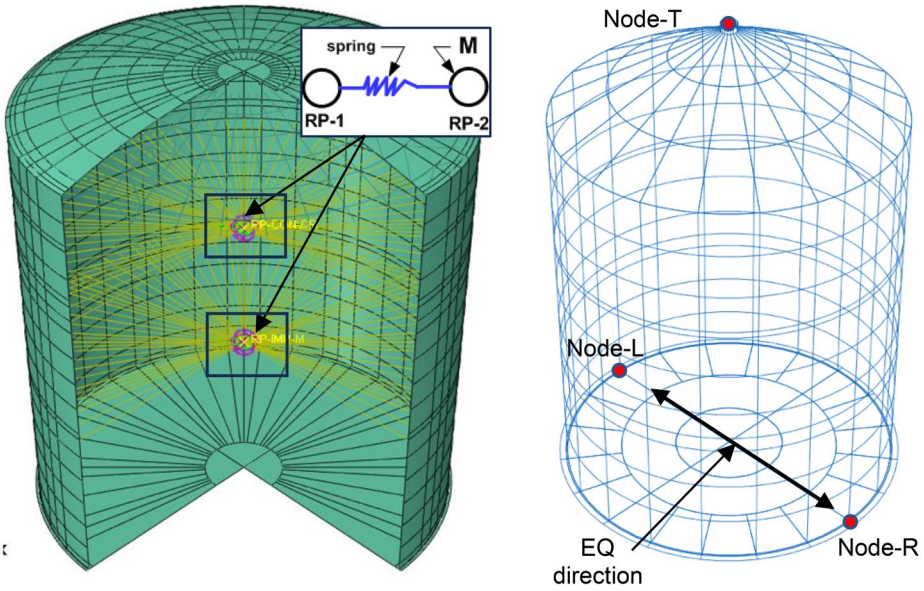


Fig. 11 Tank (**a**) liquid masses (**b**) tank uplift and displacement monitored nodes

The vertical acceleration effects are considered as static load acting in the opposite direction of the gravity since this case is more critical for Tank-A sliding and uplifting over the foundation and for Tank-B anchorage system. The vertical seismic acceleration is taken as $0.67S_{DS}$ per the 2018 Turkish Earthquake Regulation (TER-2018) (2018), where S_{DS} is the design spectrum acceleration parameter for the tank sites for the short period. The earthquake loads are applied to the tank foundation as ground acceleration histories using the reference point controlling the rigid body motions of the tank foundation. The load combination considered according to TER-2018 is $D+1.0E_h+0.3E_v$, where D accounts for all dead loads, including liquid weight and nonstructural weights, E_h represents the horizontal seismic load, and E_v denotes the vertical seismic load acting in an upward vertical direction opposite to the gravity.

3.3 Strong ground motions selection and scaling

Nonlinear time history analyses of the tanks were performed using recorded accelerograms of eleven natural strong ground motions. Two sets of ground acceleration records given in Tables 2 and 3 were selected from the Pacific Earthquake Engineering Research (PEER) Center NGA-West2 database (2013) for Tank-A and Tank-B, respectively. The records, which have V_{s30} larger than 360 m/s, were selected based on tanks site soil classification, earthquake magnitude, rupture fault distance, and fault type. All selected records have a strike-slip fault mechanism, which correlates with the proximity of the North Anatolian Fault to the tank sites.

The earthquake records selected for Tank-A site range in moment magnitude from 6.0 to 7.1, with rupture distances spanning from 0.5 to 41.9 km. At Tank-B site, the records have moment magnitude between 6.2 and 7.7, and rupture distances from 12.6 to 53.3 km.

Table 2 Summary of earthquake ground records for Tank-A site

EQ ID	Earthquake (year)	Component	Mag.(*)	Dist.(*)	Scaling
Equation 1	Helena Montana (1935)	Caroll College	6.0	2.9	5.27
Equation 2	Victoria Mexico (1980)	Cerro Prieto	6.3	14.4	2.73
Equation 3	Morgan Hill (1984)	Coyote Lake Dam	6.2	0.5	1.10
Equation 4	Duzce Turkey (1999)	Lamont 375	7.1	3.9	2.00
Equation 5	Chi-chi Taiwan (1999)	CHY074	6.2	6.2	2.71
E6	Tottori Japan (2000)	TTR007	6.6	11.3	1.47
Equation 7	Bam Iran (2003)	Bam	6.6	1.7	1.31
Equation 8	Parkfield CA (2004)	Cholame 4 W	6.0	4.2	2.76
Equation 9	Big Bear (1992)	Fire Sta #36	6.5	41.9	5.68
Equation 10	Joshua Tree CA (1992)	Fire Sta # 36	6.1	22.0	4.99
Equation 11	Duzce Turkey (1999)	Irigm 498	7.1	3.6	2.00

(*) Mag. is moment magnitude, Dist. is distance to rupture plane in km

Table 3 Summary of earthquake ground records for Tank-B site

EQ ID	Earthquake (year)	Component	Mag.(*)	Dist.(*)	Scaling
Equation 1	Imperial Valley-06 (1979)	Cerro Prieto	6.5	15.2	3.1
Equation 2	Morgan Hill (1984)	San Justo Dam	6.2	31.9	7.4
Equation 3	Chalfant Valley-02 (1986)	Bento	6.2	21.6	3.1
Equation 4	Kocaeli-Turkey (1999)	Fatih	7.5	53.3	3.6
Equation 5	Duzce-Turkey (1999)	Mudurnu	7.1	34.3	5.7
Equation 6	Sitka-Alaska (1972)	Sitka	7.7	34.6	7.9
Equation 7	Manjil-Iran (1990)	Abbar	7.4	12.6	1.2
Equation 8	Hector Mine (1999)	Keys View	7.1	50.4	7.9
Equation 9	Chi-Chi Taiwan (1999)	CHY046	6.2	38.1	4.0
Equation 10	Kern County (1952)	Kern/Taf111	7.4	41.0	2.8
Equation 11	Parkfield (1966)	Cholame	6.2	17.6	7.8

(*) Mag. is moment magnitude, Dist. is distance to rupture plane in km

Consequently, the two sets of ground motion accelerations include both near-fault and far fault events.

The tank sites design spectra (target spectra) were developed in accordance with TER-2018. Both tank sites are characterized by dense layers of sand, gravel, and hard clay, and they are classified as site class ZC under the TER-2018 guidelines. Site Class ZC is defined by an average shear wave velocity V_{s30} ranging from 360 to 760 m/s.

Tank-A site has peak ground acceleration (PGA) of 0.556 g and peak ground velocity (PGV) of 40.7 cm/s, as per Turkey Earthquake Risk Maps provided by The Disaster and Emergency Management Presidency (AFAD 2024) for earthquake level DD2. The DD2 earthquake level, defined as the standard design earthquake, carries a 10% probability of occurrence within a 50-year timeframe and has a return period of 475 years. The site-specific 5% damped design spectrum features acceleration parameters with a short period (S_{DS}) of 1.614 g and at period of 1 s (S_{D1}) equal to 0.551 g per AFAD. The Tank-B site has PGA and PGV values of 0.426 g and 26.5 cm/s respectively, for earthquake level DD2. The site-specific 5% damped design spectrum has a SDS of 1.219 g and S_{D1} of 0.408 g per AFAD.

The ground motions are scaled to match the target spectrum, as shown in Fig. 12. The ground accelerations were scaled using a constant scale factor across all acceleration data

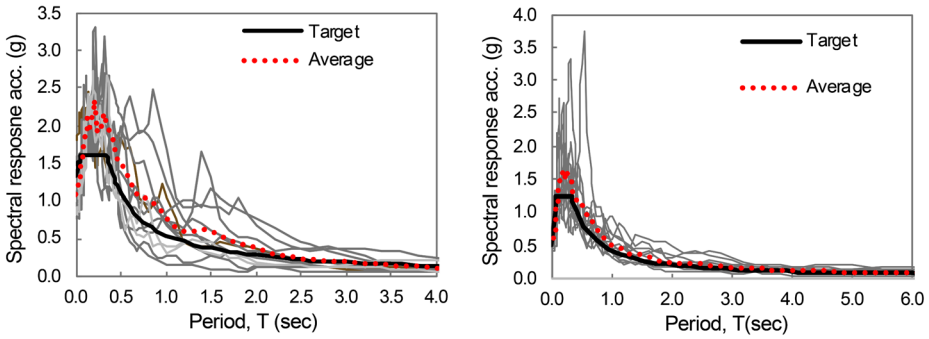


Fig. 12 Acceleration response spectra for the selected earthquakes (**a**) Tank-A (**b**)Tank-B sites

to ensure that the average response spectra of all motions remain above the target spectrum within the period range of $0.2T_i$ and $1.0T_c$ for each tank site. The TER-2018 recommends scaling ground motions across a period range of $0.2T$ to $1.5T$, where T is the natural period of fundamental mode of the structure. The upper limit on the period is intended to account for period elongation resulting from plastic deformations. However, the tank's convective period significantly exceeds the recommended upper limit of 1.5 times the structure natural period. Therefore, the upper limit of $1.5T$ is replaced with tank convective period.

4 Analysis results and discussion

4.1 Self-anchored tank (Tank-A) results

A summary of the seismic performance of Tank-A is given in Table 4. To assess the seismic performance of Tank-A, relative horizontal displacements at the tank top, tank base sliding and base uplift histories, and equivalent plastic strain (PEEQ) were monitored. Tank-A base sliding, uplift, and roof top relative lateral displacement histories are given in Fig. 13 for Eq. 9. The results show that Tank-A is susceptible to significant sliding over its foundation, with a maximum value of 92 cm and an average value of 32 cm. Although the average sliding is just under the 34 cm clearance between the tank wall and edge of its foundation, as shown in Fig. 3, the sliding observed during Eq. 3, Eq. 5, and Eq. 8 exceeds this critical threshold. This presents a significant risk of tank failure and collapse due to instability. Another potential risk is the failure of the piping system connected to the tank. The average sliding of 32 cm significantly exceeds the typical piping flexibility requirement recommended by API 650 for self-anchored tanks, which is approximately 13 cm.

Liquid storage tanks are allowed to be designed as self-anchored if their anchorage ratio "J " is less than 1.54 according to API 650. The calculated anchorage ratio for Tank-A is approximately 5.2, indicating that the tank should have been designed as a mechanically anchored tank. The anchorage ratio is calculated by the following API 650 equation:

Table 4 Tank-A seismic performance summary

EQ ID	Sliding (cm)	Top displacement (cm)	Uplift-L (cm)	Uplift-*R* (cm)	PEEQ (%)
Equation 1	32	14	5	8	0.3
Equation 2	15	28	19	12	1.0
Equation 3	47	52	22	33	3.2
Equation 4	4	12	4	8	0.1
Equation 5	92	75	29	50	11.0
Equation 6	9	11	7	6	0.2
Equation 7	21	24	15	11	0.8
Equation 8	84	42	12	24	1.2
Equation 9	25	24	14	17	2.5
Equation 10	7	13	9	8	0.1
Equation 11	11	15	9	8	0.2
Max.	92	75	29	50	11.0
Avrg.	32	28	13	17	1.9

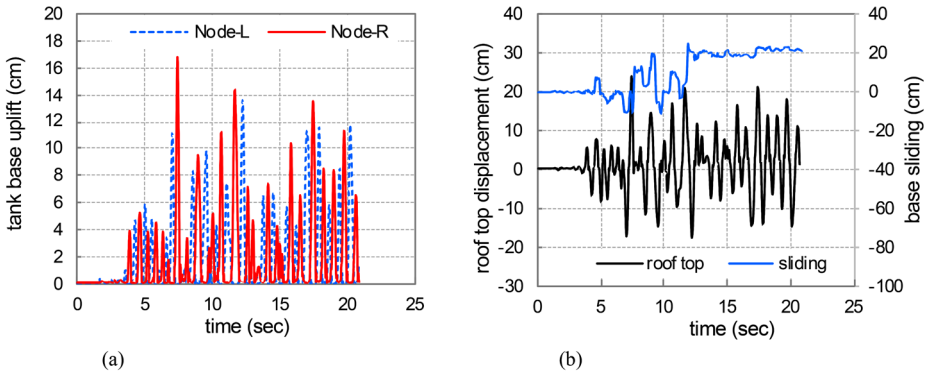


Fig. 13 Tank-A (**a**) base uplift (**b**) roof top relative lateral displacement and base sliding histories (Eq. 9)

$$J = \frac{M_{rw}}{D^2\left[\left(\frac{W_s}{\pi D} + w_{rs}\right)(1 - 0.4A_v) + w_a - 0.4w_{int}\right]} \tag{4}$$

Where M_{rw} is overturning ringwall moment, W_s is total weight of tank shell, A_v is vertical earthquake acceleration parameter, w_a is force resisting uplift in annular region, and w_{int} is design uplift load due to product pressure per unit circumferential length. The maximum and average tank base uplift values are 50 cm and 18 cm, respectively. These significant base uplift values indicate a high probability of piping and piping connection failure under seismic load. The time history analyses performed for Tank-A do not indicate any instances of tank overturning failure during any earthquake events. The factor of safety for tank overturning under Eq. 5, during which Tank-A experienced the largest base sliding and uplift, is approximately 2.4.

The tank steel plate damage and plasticity are assessed using PEEQ values, which are scalar measure of equivalent strain providing insight into the steel material susceptibility

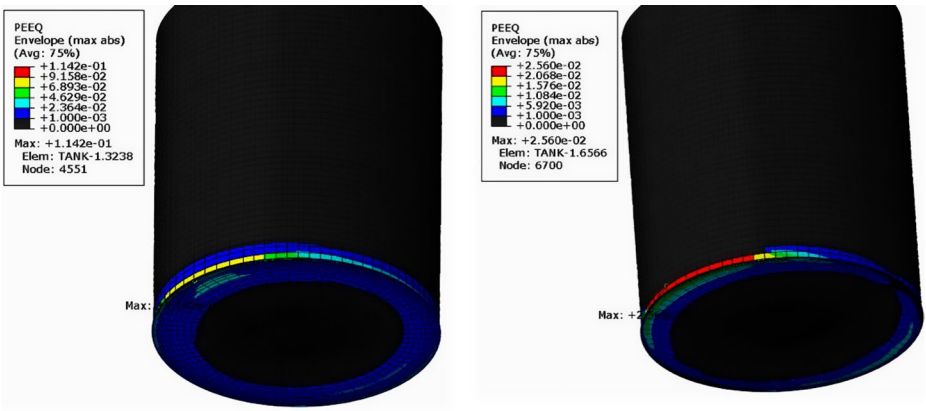


Fig. 14 Tank-A PEEQ strain contours at the end of (**a**) Eq. 5 and (**b**) Eq. 9

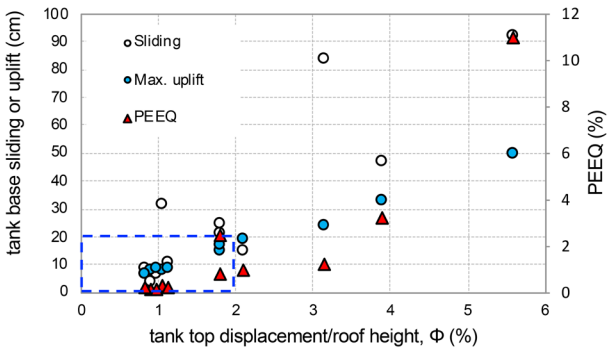


Fig. 15 Tank-A top roof displacement, base sliding, base uplift, and PEEQ comparison

to rupture. The tank experienced significant yielding at tank wall-base plate connection region due to tank uplift as shown in Fig. 14. The average and maximum PEEQ values for the tank are 1.9% and 11%, respectively, as given in Table 4. Figure 15 shows relationship between tank top displacement and tank base sliding, uplift, and PEEQ. The results indicate that when the tank top displacement to roof height ratio is less than 2%, both tank sliding and uplift remain under 25 cm, and the PEEQ value remains below the critical threshold of 2.5%.

4.2 Mechanically anchored tank (Tank-B) results

The seismic performance of Tank-B is evaluated based on maximum tank base uplift, roof top lateral displacement, and maximum PEEQ plastic strain values for both tank and its anchorage system. In addition, the overturning moment used in the tank design is compared to the average overturning moment calculated from the time history analysis of the tank. A summary of tank maximum base uplift and top displacements as well as PEEQ strain values is given in Table 5. The maximum tank base uplift displacement is less than 3 mm

Table 5 Tank-B seismic performance summary

EQ ID	Uplift (mm)	roof lateral displacement (mm)	PEEQ anchor (%)	PEEQ tank (%)
Equation 1	3	27	12	0.1
Equation 2	3	23	2.4	0.1
Equation 3	3	89	3.5	0.1
Equation 4	2	17	2.4	0
Equation 5	1	11	0.1	0
Equation 6	1	10	0.1	0
Equation 7	1	12	0.2	0
Equation 8	2	19	1.0	0
Equation 9	2	14	0.5	0
Equation 10	2	15	0.4	0
Equation 11	3	25	13	0.1
Max.	3	89	13	0.1
Avrg.	2	24	3.2	<0.1

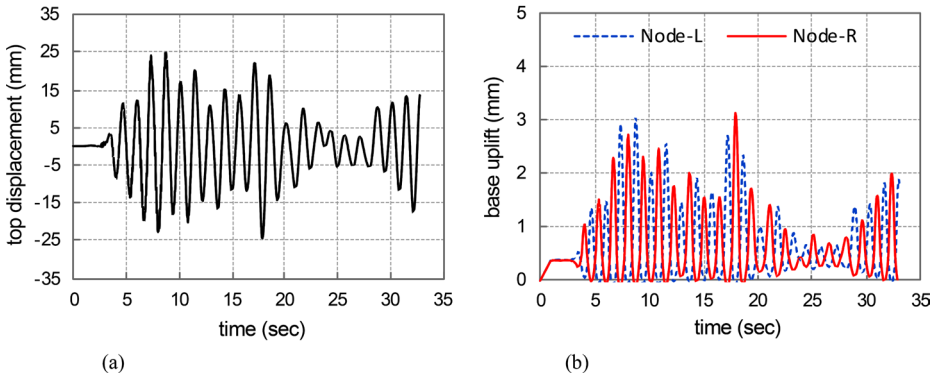


Fig. 16 Tank-B (**a**) roof top relative lateral (**b**) base uplift displacement histories (Eq. 11)

due to effective restraint provided by the tank anchorage system. The average tank roof relative lateral displacement is 24 mm, which is acceptable for piping flexibility as per API 650 standards. Tank base uplift and roof lateral relative displacement histories are given in Fig. 16 for reference.

The tank anchor system experienced yielding (PEEQ values larger than zero) under all earthquakes considered. The average PEEQ strain value for the anchors is 3.2%, indicating a moderate level of steel plastic strain and structural damage. The anchorage PEEQ strain values exceeded 2% in only five out of the total eleven earthquakes considered. The tank itself showed minimal to no steel yielding, with an average PEEQ strain value of less than 0.1%. Figure 17 shows PEEQ contours at the end of analysis for the tank under Eq. 1. The results show that anchorage plates in the direction of ground motions as well as those located at the orthogonal direction yielded showing that the anchorage damage due to both overturning moment and tank base shear forces.

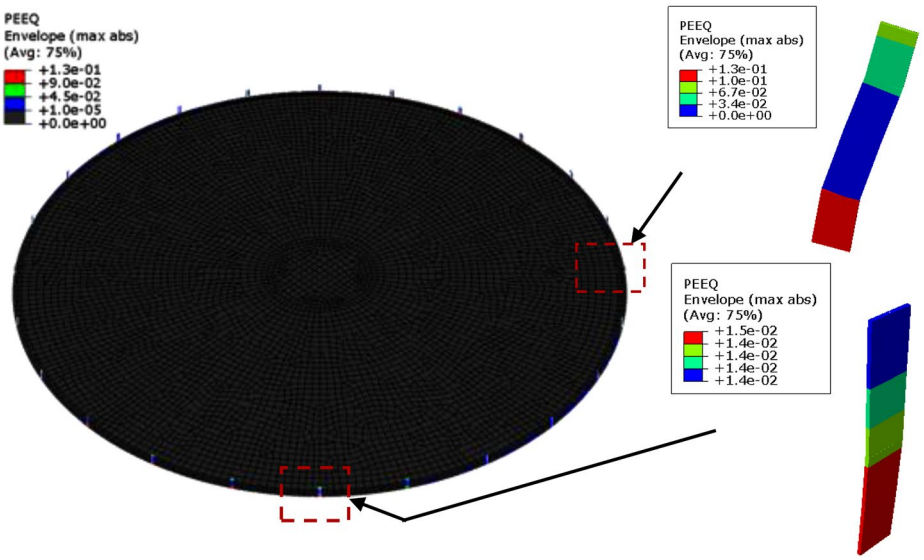


Fig. 17 Tank-B anchors PEEQ strain contours at the end of Eq. 1

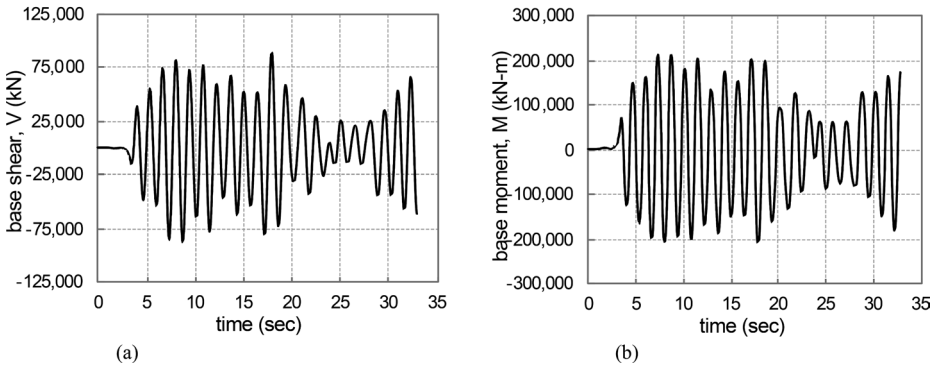


Fig. 18 Tank-B (**a**) base shear and (**b**) base overturning moment histories (Eq. 11)

The tank base overturning moment and shear loads were monitored for all chosen ground motions. In Fig. 18, the tank base shear and overturning moment histories during Eq. 11 are shown. The average overturning moment is 205,227 kN-m, which is only 80% of the overturning moment used for the tank design. In addition, it should be noted that the tank has been designed using allowable stress design approach. In summary, the analysis results show that Tank-B has satisfactory seismic performance for the specified site class and seismic level, and seismic performance of the tank is primarily controlled by the effectiveness of its anchorage system rather than the tank structure itself.

5 Conclusions

In this study, the seismic performance of two industrial at-grade liquid-storage tanks is investigated. The first tank is self-anchored and has been in service for 44 years, while the other tank is mechanically anchored and has been in service for 50 years. The tanks are located in the high seismic Marmara region of Turkey. Nonlinear time-history analyses were performed for each tank using eleven recorded ground motions selected specific to the tank sites. The seismic analyses account for both material and geometric nonlinearity, which is attributed to tank geometric imperfections and tank displacement under seismic loads. Based on the analyses results presented, the main conclusions are as follows.

1. Self-anchored tank is susceptible to significant sliding over its foundation, with a maximum value of 92 cm and an average value of 32 cm. This presents a significant risk of tank failure and collapse due to instability.
2. Self-anchored tank average base sliding of 32 cm and base uplift of 18 cm significantly exceed the typical piping flexibility capacity, and this possess a potential risk for failure of piping system, which can result in spill of liquid content.
3. The calculated anchorage ratio for self-anchored tank is 5.2, which indicates that the tank should have been designed as a mechanically anchored tank.
4. The self-anchored tank experienced significant yielding at tank wall-base plate connection region due to tank base uplift. The average equivalent plastic strain PEEQ for the tank is 1.9%.
5. For mechanically anchored tank, the maximum tank base uplift is negligible due to effective restraint provided by the tank anchorage. The average tank roof relative lateral displacement is 24 mm, which is acceptable for piping flexibility per API 650 standards.
6. The mechanically anchored tank anchorage system experienced yielding under all earthquakes considered. The average PEEQ strain value for the anchors is 3.2%, indicating a moderate level of steel plastic strain and structural damage. However, the tank itself showed minimal to no steel yielding, with an average PEEQ strain value of less than 0.1%. Therefore, it is crucial to prioritize the assessment of tank anchorages in post-earthquake damage evaluation when a comprehensive assessment is hindered due to tank insulation.
7. The average anchored tank overturning moment is approximately 80% of the overturning moment considered in the tank design.

Author contributions The manuscript was written by the author, who approves the final manuscript.

Funding The author declares that no funds, grants, or other support were received during the preparation of this manuscript.
Open access funding provided by the Scientific and Technological Research Council of Türkiye (TÜBİTAK).

Data availability The datasets generated during and/or analysed during the current study are available from the corresponding author on reasonable request.

Code availability ABAQUS is the only software employed for this research. The code is available from Dassault Systemes.

Declarations

Competing interests The author has no relevant financial or non-financial interests to disclose.

Open Access This article is licensed under a Creative Commons Attribution 4.0 International License, which permits use, sharing, adaptation, distribution and reproduction in any medium or format, as long as you give appropriate credit to the original author(s) and the source, provide a link to the Creative Commons licence, and indicate if changes were made. The images or other third party material in this article are included in the article's Creative Commons licence, unless indicated otherwise in a credit line to the material. If material is not included in the article's Creative Commons licence and your intended use is not permitted by statutory regulation or exceeds the permitted use, you will need to obtain permission directly from the copyright holder. To view a copy of this licence, visit http://creativecommons.org/licenses/by/4.0/.

References

Abaqus (2021) ABAQUS documentation, Ver. 6.21. Dassault Systems

Afad (2024) Disaster and emergency management presidency. Ministry of interior, Ankara. https://tdth.afa.gov.tr/TDTH/main.xhtml. Accessed 05/01/2024

Altunsu E, Güneş O, Öztürk S, Sorosh S, Sarı A, Beeson ST (2024) Investigating the structural damage in Hatay province after Kahramanmaraş-Türkiye earthquake sequences. Eng Fail Anal 157. https://doi.org/10.1016/j.engfailanal.2023.107857

API 620 (1970) Recommended rules for design and construction of large, welded, low-pressure storage tanks. American petroleum institute, Washington D.C.

API 650 (2020) Welded tanks for oil storage. American petroleum institute, Washington D.C.

API 653 (2014) Tank inspection, repair, alteration, and reconstruction. American petroleum institute, Washington D.C.

Bakalis K, Karameros SA (2021) Uplift mechanics of unanchored liquid storage tanks subjected to lateral earthquake loading. Thin-Walled Struct 158. https://doi.org/10.1016/j.tws.2020.107145

Caprinozzi S, Paolacci F, Dolšek M (2020) Seismic risk assessment of liquid overtopping in a steel storage tank equipped with a single deck floating roof. J Loss Prev Process Ind 67. https://doi.org/10.1016/j.jlp.2020.104269

Çelik Aİ, Köse MM (2020) Dynamic buckling analysis of cylindrical steel water storage tanks subjected to Kobe earthquake loading. Steel Constr 13(2):128–138. https://doi.org/10.1002/stco.201900003

Chang JI, Lin CC (2006) A study of storage tank accidents. J Loss Prev Process Ind 19(1):51–59. https://doi.org/10.1016/j.jlp.2005.05.015

Chaulagain NR, Sun CH, Kim I (2018) Seismic behavior of liquid storage tanks using complex and simple analytical models. J Earthq Eng Soc Korea. https://api.semanticscholar.org/CorpusID:115284330

Girgin S (2011) The natech events during the 17 August 1999 Kocaeli earthquake: Aftermath and lessons learned. Nat Hazards Earth Syst Sci 11(4):1129–1140. https://doi.org/10.5194/nhess-11-1129-2011

Goudarzi MA (2020) Numerical investigation on accuracy of mass spring models for cylindrical tanks under seismic excitation. https://api.semanticscholar.org/CorpusID:214789773

Haroun MA (1983) Behavior of unanchored oil storage tanks: Imperial valley earthquake. https://api.semanticscholar.org/CorpusID:109885030

Haroun MA, Housner GW (1981) Seismic design of liquid storage tanks. J Tech Councils ASCE 107:191–207

Hernandez D, Larkin TJ, Chouw N (2021) Evaluation of the adequacy of a spring-mass model in analyses of liquid sloshing in anchored storage tanks. Earthq Eng Struct Dynamics 50:3916–3935

Housner GW (1957) Dynamic pressures on accelerated fluid containers. Bull Seismol Soc Am 47(1):15–35

Housner GW (1963) The dynamic behavior of water tanks. Bull Seismol Soc Am 53:381–387

Jacobsen LS (1949) Impulsive hydrodynamics of fluid inside a cylindrical tank and of fluid surrounding a cylindrical pier*. Bull Seismol Soc Am 39(3):189–204. https://doi.org/10.1785/BSSA0390030189

Kalantari A, Nikoomanesh MR, Goudarzi MA (2019) Applicability of mass-spring models for seismically isolated liquid storage tanks. J Earthq Tsunami 13(01). https://doi.org/10.1142/S1793431119500027

Malhotra PK (1995) Base uplifting analysis of flexibly supported liquid-storage tanks. Earthquake Eng Struct Dynam 24:1591–1607

Malhotra P, Wenk T, Wieland M (2000) Simple procedure for seismic analysis of liquid-storage tanks. Struct Eng Int 10(3):197–201. https://doi.org/10.2749/101686600780481509

Manos GC, Clough RW (1985) Tank damage during the may 1983 coalinga earthquake. Earthquake Eng Struct Dynam 13:449–466
Men J, Chen G, Reniers G, Wu Y, Huang H (2024) Experimental and numerical study on earthquake-fire coupling failure mechanism of steel cylindrical tanks. Reliab Eng Syst Saf 245. https://doi.org/10.1016/j.ress.2024.110016
Ormeño M, Larkin TJ, Chouw N (2015) The effect of seismic uplift on the shell stresses of liquid-storage tanks. Earthquake Eng Struct Dynam 44:1979–1996
Ormeño M, Larkin T, Chouw N (2019) Experimental study of the effect of a flexible base on the seismic response of a liquid storage tank. Thin-Walled Struct 139:334–346. https://doi.org/10.1016/j.tws.2019.03.013
Ozdemir Z, Souli M, Fahjan YM (2010) Application of nonlinear fluid–structure interaction methods to seismic analysis of anchored and unanchored tanks. Eng Struct 32(2):409–423. https://doi.org/10.1016/j.engstruct.2009.10.004
PEER (2013) NGA-West2 database. Pacific Earthquake Engineering Research Center, Univ. California, Berkeley, CA. Accessed 15/09/2023
Rawat A, Matsagar V (2022) Seismic analysis of liquid storage tank using oblate spheroid base isolation system based on rolling friction. Int J Non-Linear Mech 147. https://doi.org/10.1016/j.ijnonlinmec.2022.104186
Scawthorn C, Johnson GS (2000) Preliminary report Kocaeli (Izmit) earthquake of 17 August 1999. Eng Struct 22(7):727–745
Sezen H, Whittaker AS (2004) Performance of industrial facilities during the 1999, Kocaeli, Turkey earthquake. 13th world conference on earthquake engineering, Vancouver, B.C., Canada
Shih C, Babcock CD (1984) Buckling of oil storage tanks in SPPL tank farm during the 1979 Imperial Valley Earthquake. J Press Vessel Technology-Transactions Asme 109:249–255
Spritzer JM, Guzey S (2017) Nonlinear numerical evaluation of large open-top aboveground steel welded liquid storage tanks excited by seismic loads. Thin-Walled Struct 119:662–676. https://doi.org/10.1016/j.tws.2017.07.017
Spritzer JM, Bohra H, Guzey S (2019) Imperfection-sensitivity of unanchored aboveground open-top steel welded liquid storage tanks subjected to seismic loads. SN Appl Sci 1. https://doi.org/10.1007/s42452-019-1597-7
TER-2018 (2018) Turkish earthquake regulation. Ministry of Interior, disaster and emergency management presidency. Government of Republic of Turkiye, Ankara
Vathi M, Karamanos SA (2015) Simplified model for the seismic performance of unanchored liquid storage tanks. ASME 2015 pressure vessels and piping conference. https://doi.org/10.1115/PVP2015-45695
Veletsos AS, Auyang J (1977) Earthquake response of Liquid Storage tanks. Advances in Civil Engineering through Engineering Mechanics, ASCE, Raleigh, pp 1–24
Zhu H, Tang Z, Luo H (2023) Seismic performance of a base-isolated flexible liquid storage tank equipped with a novel rate-independent damping device. Structures 51:215–225. https://doi.org/10.1016/j.istruc.2023.03.024

Publisher's Note Springer Nature remains neutral with regard to jurisdictional claims in published maps and institutional affiliations.